(Received 24 November 2024, Accepted 3 January 2025, Scheduled 12 January 2025)

Highly Isolated and Miniaturized SIW Based Self-Quadplexing Antenna with Modified CSRR-Inspired Slots for S-Band Wireless Applications

Matta Venkata Pullarao[1,*], Singam Aruna[1], and Kethavathu Srinivasa Naik[2]

[1] *Department of Electronics and Communication Engineering, AU College of Engineering, Andhra University, Visakhapatnam, India*
[2] *Department of Electronics and Communication Engineering, Vignans Institute of Information Technology Visakhapatnam, India*

ABSTRACT: This paper presents a highly miniaturized self-quadplexing antenna based on a quarter-mode substrate integrated waveguide. The miniaturization of the antenna is achieved by utilizing a pair of complementary split-ring resonator-inspired slots. The quadplexing characteristics of the antenna are achieved by varying the width of the inner CSRR-shaped slot. The antenna is designed to resonate at four distinct frequencies: 2.09 GHz, 2.18 GHz, 2.26 GHz, and 2.36 GHz. It demonstrates a minimum port isolation exceeding 32.6 dB between the ports. Additionally, this self-quadplexing antenna offers frequency tunability and maintains a unidirectional radiation pattern across the designated operating frequencies. The antenna's simulated and measured gains are 5.32 dBi (5.44 dBi), 5.58 dBi (5.42 dBi), 5.41 dBi (5.15 dBi), and 5.18 dBi (5.26 dBi). The design supports independent frequency tunability through the activation of four ports, with a compact size of 0.037 λ_0^2, where λ_0 is determined at lowest resonant frequency. These features indicate the antenna's suitability for S-band applications.

1. INTRODUCTION

The advancement of modern wireless communication systems has significantly increased the demand for planar, low-profile, multi-band antennas. Integrating multiple antennas onto a single platform is essential to accommodate the various requirements of different frequency bands. These antennas are finely tuned to meet the specific needs of contemporary communication systems. However, practical implementations often require external multiplexers for frequency band selection, which adds to the system's spatial footprint. To overcome this challenge, innovative antenna topologies with inherent multiplexing capabilities have been developed, enabling multi-band functionality without external multiplexers. Additionally, the ongoing trend toward miniaturization requires these devices to remain compact. Substrate Integrated Waveguide (SIW) technology provides an effective solution for reducing antenna system size [1–3], offering further benefits like improved isolation between ports, enhanced performance characteristics [4–6], and seamless integration with existing platforms [7–10]. Integrating SIW technology with self-multiplexing antennas presents a promising approach to achieving compactness alongside improved performance in modern wireless systems.

A key consideration in the design of self-multiplexing SIW antennas is miniaturization, which is essential for integration into compact and space-constrained applications. Miniaturized antennas facilitate efficient multi-band functionality within a smaller footprint, meeting the needs of modern devices. Another crucial factor is the frequency ratio between operational bands. A smaller frequency ratio allows for closer spacing of different frequency bands, enabling more efficient use of available sub-bands and providing additional channels within the target range. This compact frequency spacing also improves data rate capacity, optimizing the limited frequency spectrum. The demand for multiband antennas with small frequency ratios continues to grow, as they support simultaneous operation across multiple frequencies within the same band, maximizing spectral efficiency. In recent years, significant research has focused on the design of antennas incorporating SIW technology, with many dual-band [11–16] and triple-band [17–21] configurations being proposed. Additionally, SIW-based self-quadplexing antennas have been developed using modes such as half-mode SIW [22, 23] and quarter-mode SIW [24, 25]. Various slot shapes have been explored in these designs, including V-shaped [26, 27], U-shaped [28], unequal patch resonators [29], T-shaped slots [30], swastik-shaped slots [31], combination of 3 different slots (rectangular-shaped slot, V-shaped slot and annular Bowtie slot) [32].

Achieving miniaturization with high isolation becomes progressively challenging as the number of ports in quadplexing antennas increases, compared to simpler diplexing and triplexing configurations. For example, a self-quadplexing antenna in [23] utilized V-shaped slots to achieve a notable isolation of 30.5 dB with a frequency ratio of 1.46, but required an electrical size of $0.42\lambda_0^2$. Similarly, by employing V-shaped slots in [27], an isolation of 22 dB with a frequency ratio of 1.34 was obtained, although with a larger electrical size of $0.81\lambda_0^2$. Additionally, the antenna design in [22] used U-shaped slots to

* Corresponding author: Matta Venkata Pullarao (venkatpullaraomatta@gmail.com).

reach a high isolation of 32.5 dB with an increased frequency ratio of 2.63. In contrast, the designs presented in [27] and [30] achieved lower frequency ratios of 1.34 and 1.38, respectively, accompanied by limited isolation levels of 22 dB and 26 dB. While these antenna structures demonstrate commendable performance characteristics, they often confront trade-offs—either exhibiting a higher frequency ratio with increased size or a lower frequency ratio with reduced isolation. As a result, designing a self-quadplexing antenna that combines high isolation, a low frequency ratio, compact size, and stable performance remains a significant challenge.

In this paper, a self-quadplexing antenna based on Substrate Integrated Waveguide technology, featuring Quarter-Mode SIW cavities is introduced. The design incorporates pairs of CSRR-inspired slots with varying widths, the resonating elements operates at four distinct frequencies 2.09 GHz, 2.18 GHz, 2.26 GHz, and 2.36 GHz and obtained self-quadplexing functionality. One notable aspect of the antenna is its ability to independently adjust each frequency band by varying the width of selected CSRR-shaped slots. This approach offers several advantages, including substantial miniaturization, strong isolation between adjacent ports without additional decoupling components, a small frequency ratio, and high gain. These features make the antenna a strong candidate for deployment in modern wireless communication systems.

2. SELF-QUADPLEXING ANTENNA DESIGN AND ANALYSIS

Figures 1(a) and (b) illustrate the top and side views of the self-quadplexing antenna, respectively. The middle substrate layer is constructed from Rogers RT/Duroid 5870 with a thickness of 0.787 mm. Both the top and bottom metallic layers are composed of copper, with each layer having a thickness of 0.035 mm. The optimized geometrical parameters are as follows: L_{eff} = 26 mm, w_1 = 4 mm, w_2 = 3 mm, w_3 = 2 mm, and w_4 = 1 mm.

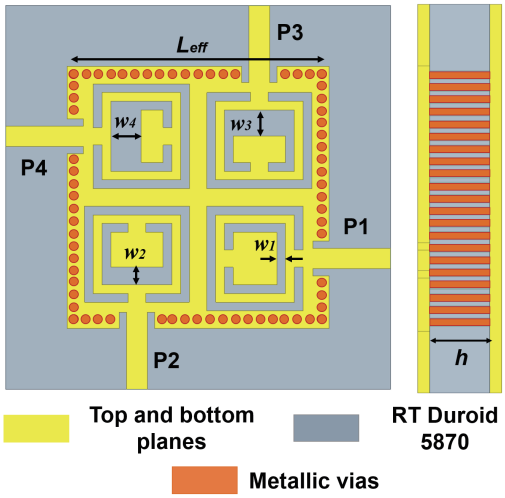

FIGURE 1. (a) Schematic-view and (b) side-view of the proposed antenna.

The design methodology of the proposed self-quadplexing antenna is shown in Fig. 2 is as follows:

1. Design a square SIW cavity (Structure 1) with four microstrip feed lines to each side of the square cavity.
2. To obtain the miniaturization, design four quarter-mode cavity resonators by introducing a pair of CSRR-inspired slots at the four corners on the top plane of the square cavity.
3. To enable self-quadplexing characteristics, adjust the dimensions of the width of the inner CSRR-shaped slot to obtain the resonant frequencies with high isolation suitable for different wireless standards and applications.
4. Assess the performance of the self-quadplexing antenna through electromagnetic and circuit model simulations, prototyping, and experimental measurements.

Initially, an SIW based SCR (Structure 1) is designed with the effective length and width of 28 mm × 28 mm with 50Ω feed lines as shown in Fig. 3. The resonant frequency of the conventional SIW square cavity resonator (SCR) for the TE_{110} can be calculated by using 1

$$f_{110}^{SCR} = \frac{c}{2\sqrt{\varepsilon_r}}\sqrt{\left(\frac{1}{l_{eff}}\right)^2 + \left(\frac{1}{w_{eff}}\right)^2} \tag{1}$$

where ϵ_r represents the relative permittivity of the substrate, and the effective length and width of the SCR can be calculated in terms of the length (l_p) and width (w_p) of the top metallic plane by using 2 and 3

$$l_{eff}^{SCR} = l_p - \frac{d^2}{0.93s} + 10\frac{d^2}{l_p} \tag{2}$$

$$w_{eff}^{SCR} = w_p - \frac{d^2}{0.93s} + 10\frac{d^2}{w_p} \tag{3}$$

To avoid the leakage losses from the SCR, the diameter of via (d) and center-to-center distance between the vias (s) can be chosen as

$$\frac{d}{\lambda_0} < 0.1, s \leq \frac{d}{0.5} \tag{4}$$

Structure 1 resonates at 5.02 GHz, which can be verified by using 1. The reflection and transmission coefficients of the SCR are shown in Fig. 3. Since the four ports are orthogonal with each other, the SCR exhibits high mutual coupling between the four ports. By loading the CSRR-shaped slots (Structure 2) with inner and outer side lengths of 10 mm, 12 mm, respectively, on four sides of the top plane of SCR as shown in Fig. 4(a). These slots effectively increase the antenna's electrical length and alter the distribution of surface currents. Additionally, the CSRR slots enhance the inductance and introduce capacitive coupling due to their geometry and positioning, which in turn lowers the resonant frequency. It can be observed from Fig. 5(a) that there is a shift in resonant frequency

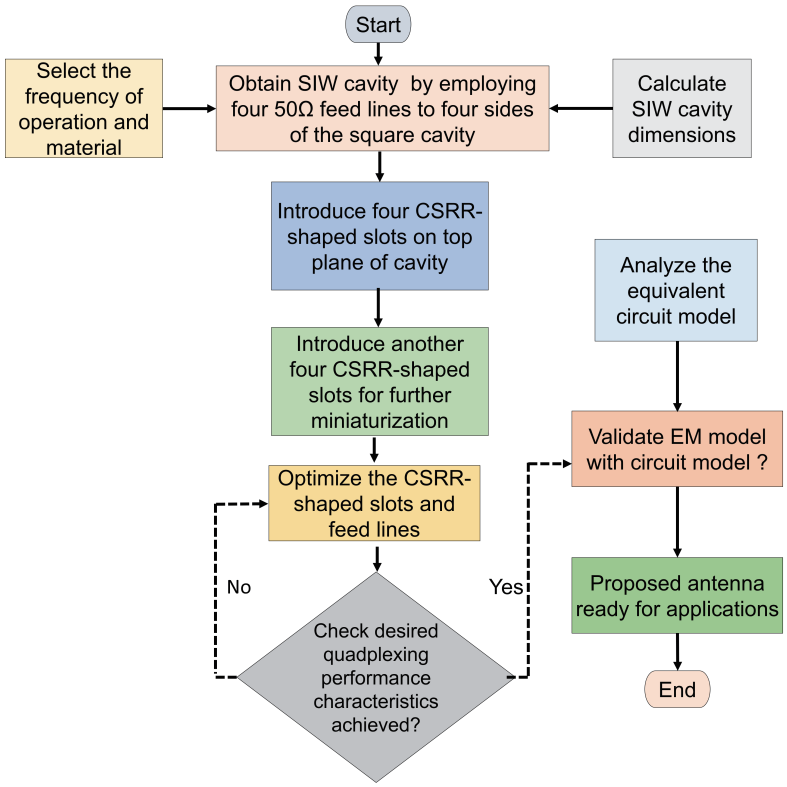

FIGURE 2. Design flowchart of the proposed self-quadplexing SIW antenna.

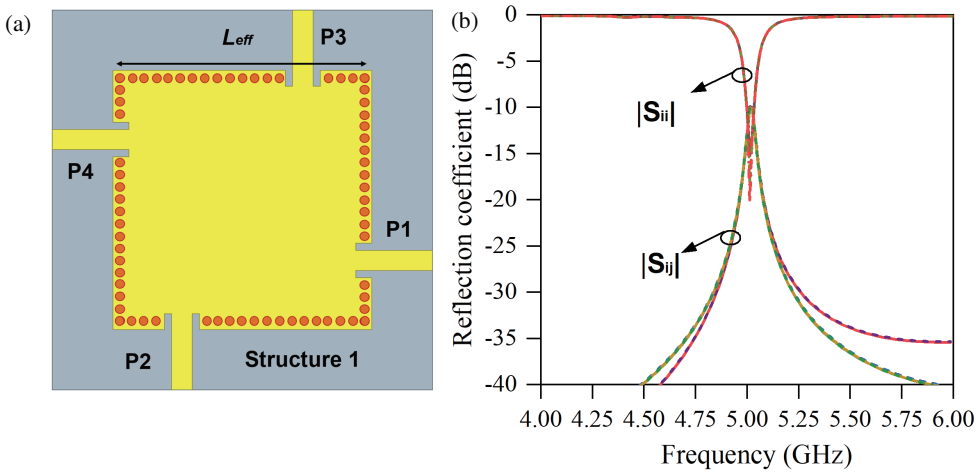

FIGURE 3. (a) Design of the square cavity resonator. (b) Reflection coefficients of the SCR.

of the antenna from 5.02 GHz to 2.82 GHz, and a reduction in frequency of 43.82% is obtained. In order to further achieve miniaturization, an additional CSRR-shaped slot (Structure 3), with inner and outer side lengths of 6 mm and 8 mm, respectively, is incorporated on the top metallic plane, as shown in Fig. 4(b). Structure 3 resonates at 2.1 GHz, achieving a miniaturization of 58.17% from 5.02 GHz to 2.1 GHz, as depicted in Fig. 5(b). The widths of the inner square rings of the second CSRR-shaped slots on the four sides are varied to obtain the self-quadplexing characteristics of the antenna (Structure 3), as shown in Fig. 4(c). The quadplexing antenna resonates at four distinct frequencies: 2.09 GHz, 2.18 GHz, 2.26 GHz, and 2.36 GHz. These slots are strategically designed and precisely positioned at the four corners of the square cavity to suppress mutual coupling. By varying the widths of the inner rings, there is low mutual coupling between the four ports, and the antenna achieved an isolation of 32.6 dB, as shown in Fig. 5(c). When the dimensions of the cavity are fixed, the introduction of CSRRs within the SIW structure plays a pivotal role in scaling the frequency bands. CSRRs effectively introduce localized

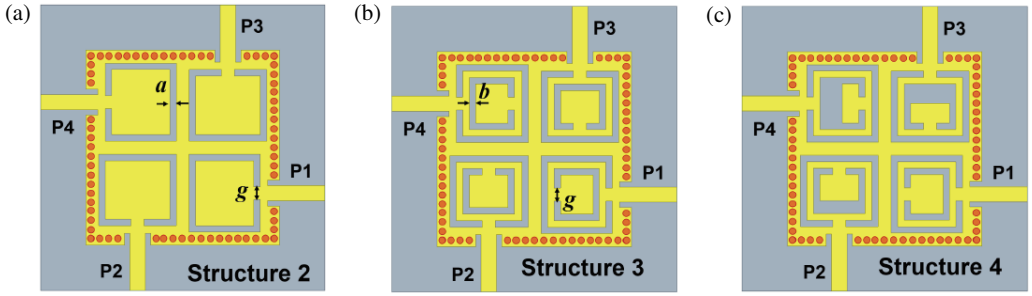

FIGURE 4. Design steps of the proposed self-quadplexing antenna. (a) Structure 2. (b) Structure 3. (c) Structure 4.

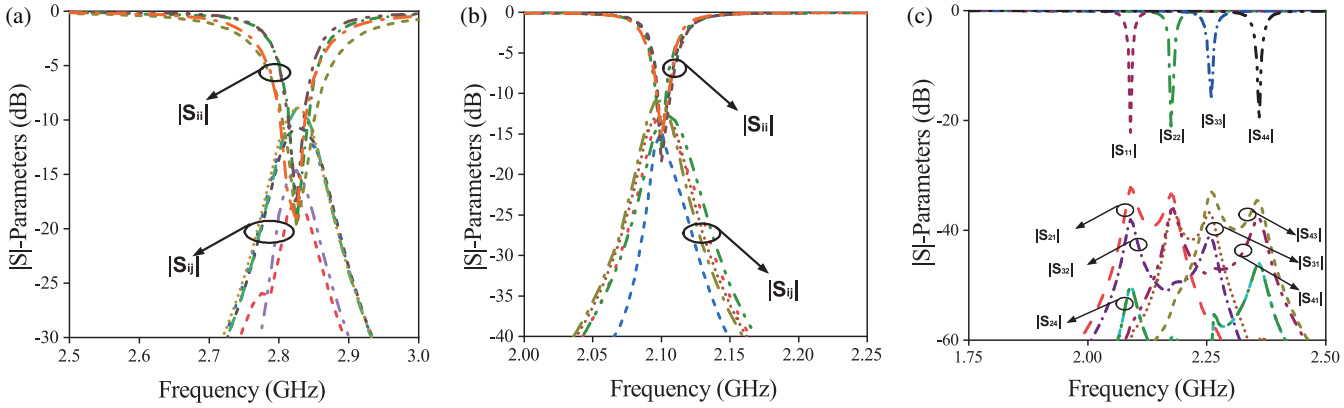

FIGURE 5. $|S|$-parameters of (a) Structure 2. (b) Structure 3. (c) Structure 4.

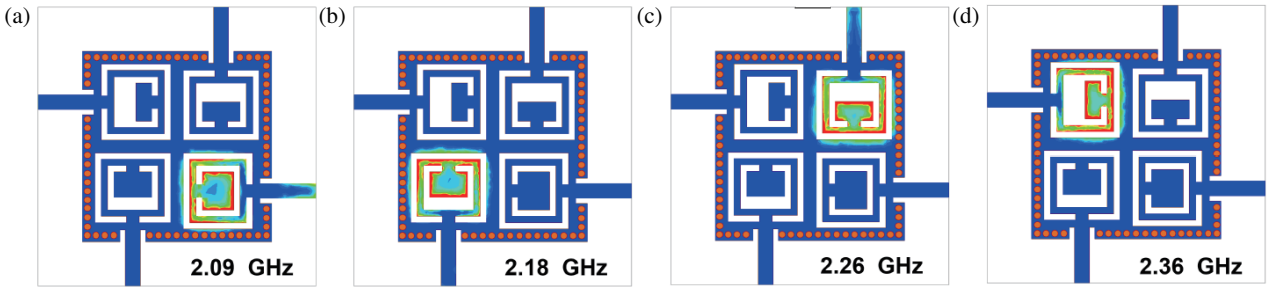

FIGURE 6. Electric field distributions of proposed antenna at four different resonant frequencies (a) $f_1 = 2.09$ GHz, (b) $f_2 = 2.18$ GHz, (c) $f_3 = 2.26$ GHz, and (d) $f_4 = 2.36$ GHz.

inductive and capacitive effects, which modify the electromagnetic field distribution within the cavity. By adjusting the size, shape, and placement of the CSRRs, the resonant frequencies can be precisely tuned without altering the overall cavity dimensions. This makes them particularly effective in achieving miniaturization and enhancing the frequency-selective behavior of SIW-based antennas, providing flexibility in designing for specific frequency bands while maintaining the compactness.

To understand the physical mechanism of the self-quadplexing antenna, the electric field distribution at the four resonant frequencies is illustrated in Fig. 6. In the self-quadplexing antenna, the electric fields are concentrated near the edges of the CSRR-shaped slots, a result of the resonant behavior of these slots. This design creates high-intensity electric fields along the slot boundaries, as the slots act as resonators that enhance the electromagnetic field in their immediate surroundings. This field confinement stems from both the geometric configuration of the slots and their interaction with the excited ports, which enhances the local field intensity near the slot edges. Additionally, to elucidate the operational concept of the self-quadplexing antenna, an equivalent circuit model has been developed, as shown in Fig. 7.

Each of the resonating elements is represented by a parallel RLC network shown in Fig. 7 which can be expressed as R_1, R_2, R_3, R_4, L_1, L_2, L_3, L_4, C_1, C_2, C_3, and C_4 for the corresponding ports 1, 2, 3, and 4, respectively. The gaps between the resonating elements are represented as C'_1, C'_2, C'_3, and C'_4, and the coupling between the resonating elements represented as M_{12}, M_{23}, M_{34}, and M_{41} are also modeled using

TABLE 1. Parameters of circuit model of the proposed antenna.

R_1	221 Ω	R_3	239 Ω	C'_1	3.92 pF	L_{23}	12.61 nH
L_1	1.56 nH	L_3	2.08 nH	C'_2	2.57 pF	C_{23}	6.45 pF
C_1	0.011 pF	C_3	0.02 pF	C'_3	2.57 pF	L_{34}	12.91 nH
R_2	210 Ω	R_4	230 Ω	C'_4	2.57 pF	C_{34}	12.45 pF
L_2	2.08 nH	L_4	1.915 nH	L_{12}	13.8 nH	L_{41}	12.91 nH
C_2	0.084 pF	C_4	0.016 pF	C_{12}	9.15 pF	C_{41}	12.45 pF

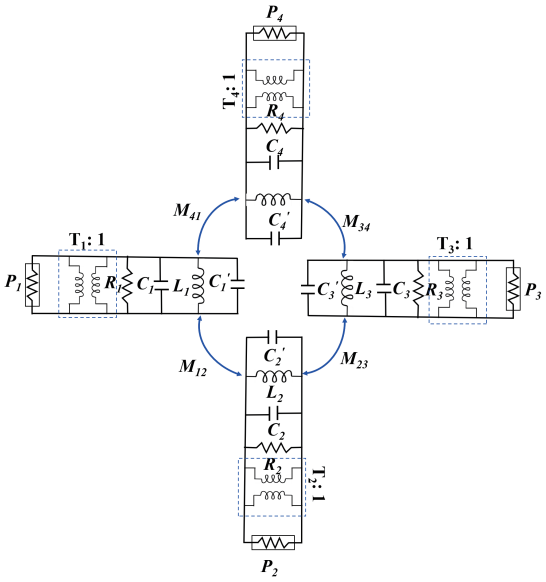

FIGURE 7. Equivalent circuit model of the proposed quadplexing antenna.

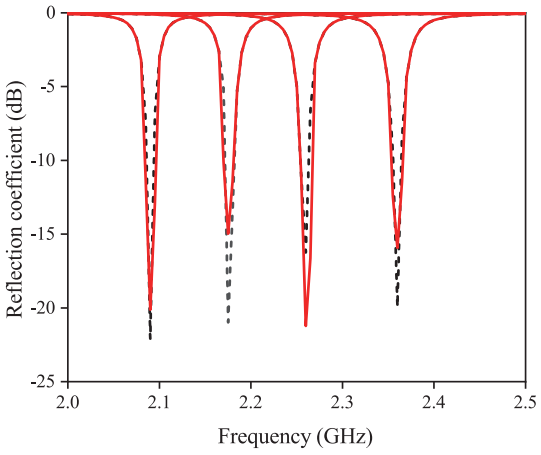

FIGURE 8. Simulated and circuit model reflection coefficients.

the series inductance and capacitance, namely (L_{12}, C_{12}), (L_{23}, C_{23}), (L_{34}, C_{34}), and (L_{41}, C_{41}), respectively. The impedance matching between the microstrip feed line and radiating elements is provided by using a transformer. The optimized parameters are listed in Table 1. The reflection coefficients of the simulated and circuit model of the self-quadplexing antenna is shown in Fig. 8.

2.1. Tunability of the Self-Quadplexing Antenna

The frequency tunable characteristics of the proposed antenna can be obtained by varying the side width of the inner CSRR-shaped slot. By varying the widths w_1, w_2, w_3, and w_4 of the CSRR, the independent frequency tunability is achieved as shown in Fig. 9. By varying the width w_1 from 0.5 to 2.5 mm, the lowest resonant frequency can be tuned from 2.02 to 2.22 GHz as illustrated in Fig. 9(a). This shows that the width w_1 affects the lowest resonant frequency, while the other resonant frequencies remain unchanged. The second resonant frequency can be varied from 2.09 GHz to 2.42 GHz by adjusting the width w_2 from 1 to 4 mm, as shown in Fig. 9(b). Similarly, the width of the slot w_3 is varied from 1 to 5 mm, so that the frequency f_3 is varied from 2.08 GHz to 5.57 GHz, as depicted in Fig. 9(c). Lastly, Fig. 9(d) shows that the resonant frequency f_4 can be tuned from 2.14 to 2.62 GHz by adjusting the width of the slot from 1.5 to 5.5 mm. This extensive tuning range (3.78–5.89 GHz) renders the proposed antenna suitable for various wireless standards. It is important to emphasize that adjustments to one frequency band have minimal impact on the others, enabling precise and independent frequency tuning. With a broad tuning range of 2.04–2.62 GHz, the proposed antenna is well suited for various wireless standards. Additionally, the antenna achieved a low frequency ratio of 1.12 while keeping other frequencies stable, highlighting the effectiveness of its design and optimization in supporting efficient multi-band performance.

3. RESULTS AND DISCUSSION

The top view photograph of the fabricated prototype of the proposed self-quadplexing antenna is shown in Fig. 10(a). Measurements of the reflection coefficients and isolation were carried out using a Keysight E5063A two-port vector network analyzer. Reflection coefficients were obtained by exciting ports 1, 2, 3, and 4 individually, while isolation was measured between various port combinations: (1 and 2), (2 and 3), (3 and 4), (4 and 2), (4 and 1), and (4 and 3). The simulated and measured reflection coefficients, S_{11}, S_{22}, S_{33}, and S_{44}, for ports 1, 2, 3, and 4 are depicted in Fig. 10(b). The measured operating frequencies of the self-quadplexing antenna are 2.09 GHz, 2.17 GHz, 2.26 GHz, and 2.35 GHz, showing a discrepancy of less than 2% compared to the simulated resonant frequencies. Furthermore, the simulated and measured isolation values indicate that S_{21} exceeds 33 dB; S_{32} is greater than 38 dB; S_{31} surpasses 36 dB; S_{34} is above 33 dB; S_{41} is greater than 35 dB;

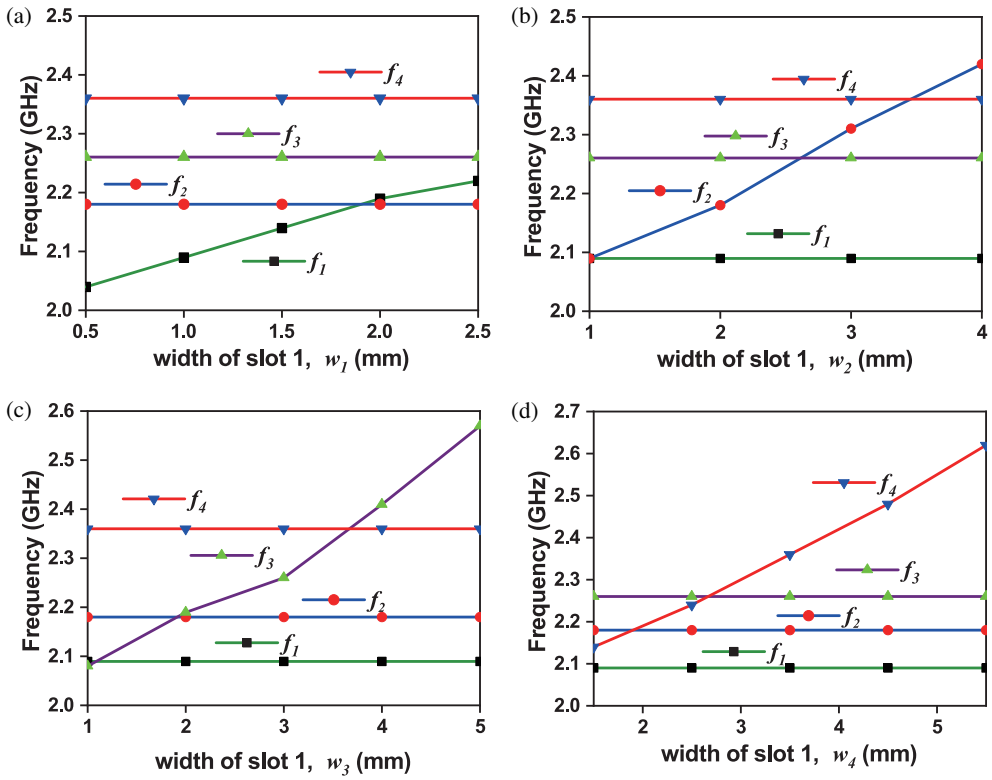

FIGURE 9. Frequency tunability of the antenna for the operating frequencies. (a) f_1, (b) f_2, (c) f_3, and (d) f_4.

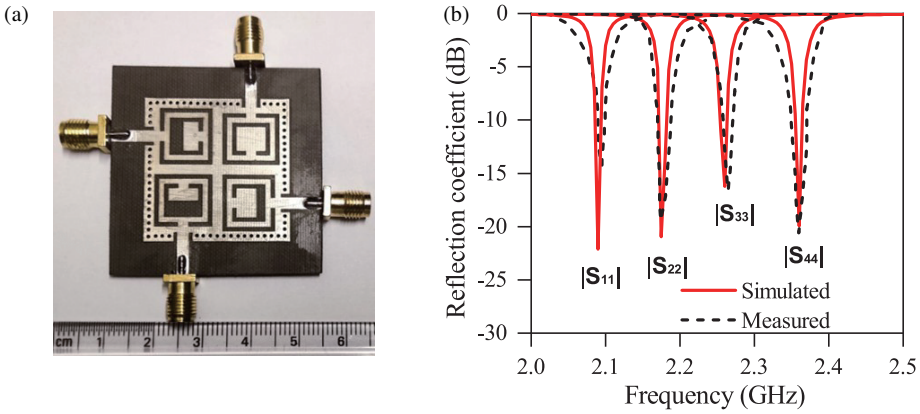

FIGURE 10. (a) Fabricated prototype. (b) Simulated and measured values of the reflection coefficient of the self-quadplexing antenna.

and S_{42} exceeds 46 dB. Thus, the overall isolation between any two ports (S_{21}, S_{31}, S_{41}, S_{23}, S_{24}, S_{34}) remains above 32.6 dB, as illustrated in Fig. 11.

The proposed self-quadplexing antenna features a directional radiation pattern, with peak radiation concentrated in the broadside direction. Fig. 12 displays the normalized radiation patterns derived from both simulated and measured results. The antenna exhibits a unidirectional radiation pattern, maintaining a cross-polarization level greater than 22 dB at its resonant frequencies. The radiation patterns for excitations at ports 1, 2, 3, and 4 are shown in Figs. 12(a)–(d), respectively. A strong alignment is observed between the measured data and electromagnetic simulation results across all frequency bands. The patterns were evaluated in the E-plane ($\phi = 0°$) and H-plane ($\phi = 90°$) for various port excitations. Both the measured and simulated radiation patterns demonstrate unidirectional and stable behavior in both planes throughout the frequency range. Additionally, the EM simulations indicate a cross-polarization level below -22.12 dB, while the measured results confirm a cross-polarization level below -22.08 dB for all frequencies. This is a significant feature, as it minimizes the effects of cross-polarization and ensures better signal quality and reduced interference between the channels, which is crucial for practical applications such as wireless communication systems. .

The gains for the antenna, based on simulations and measurements at frequencies of 2.08 GHz, 2.18 GHz, 2.26 GHz, and 2.36 GHz, are recorded as 5.32/5.44 dBi, 5.58/5.42 dBi, 5.41/5.15 dBi, and 5.18/5.26 dBi, respectively, as depicted in

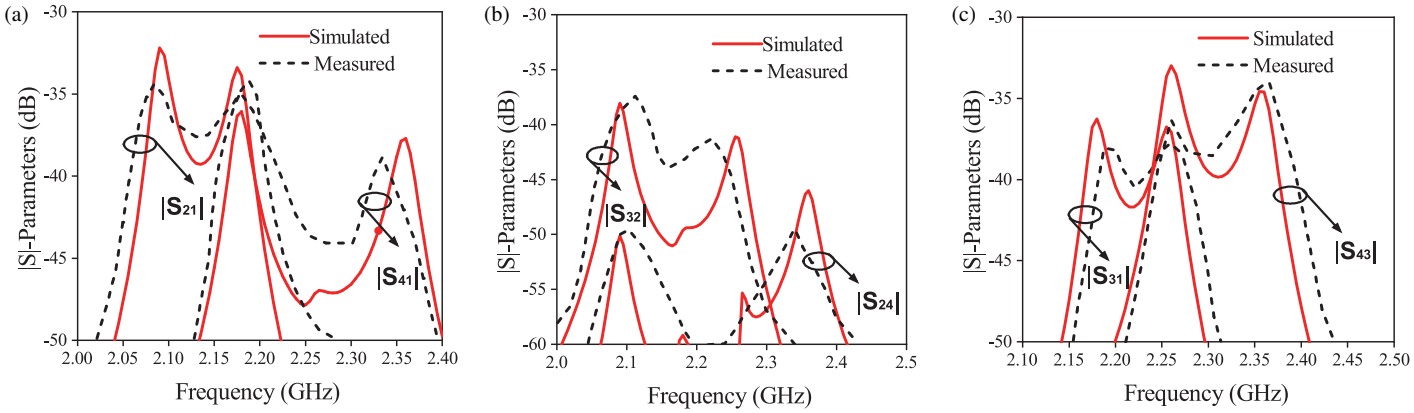

FIGURE 11. Simulated and measured values of the isolation of the self-quadplexing antenna, (a) $|S_{21}|$ and $|S_{41}|$, (b) $|S_{32}|$ and $|S_{24}|$ (c) $|S_{31}|$ and $|S_{43}|$.

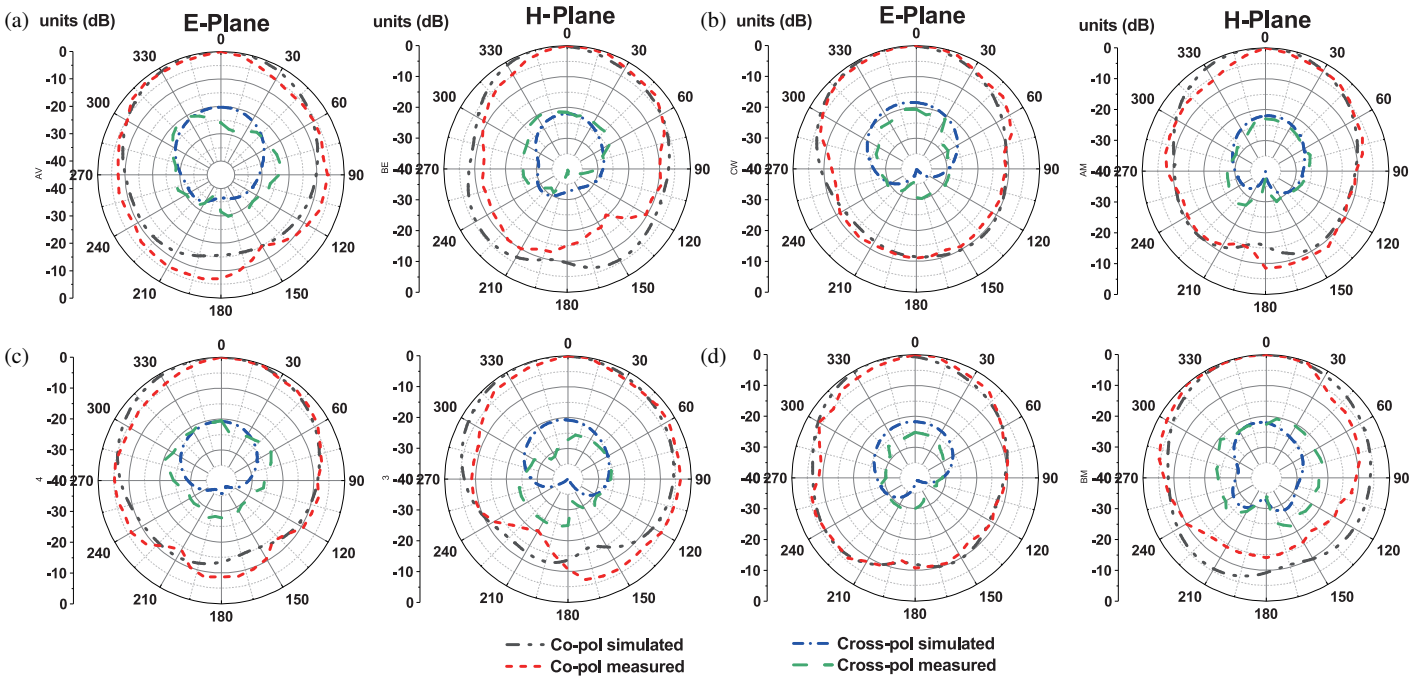

FIGURE 12. Simulated and measured normalized radiation patterns in the E-plane and H-plane.

Fig. 13. Furthermore, the self-quadplexing antenna demonstrates a radiation efficiency exceeding 80% when ports 1, 2, 3, and 4 are activated.

4. MULTIFUNCTIONAL PERFORMANCE ANALYSIS

The diversity performance of the proposed SIW-based self-quadplexing antenna was analyzed using key metrics: Envelope Correlation Coefficient (ECC), Diversity Gain (DG), and Mean Effective Gain (MEG). ECC determines the correlation between the signals received at the antenna ports. For an effective multiplexing system, ideally the ECC should be less than 0.5 [33] to ensure good diversity in radiation patterns. In the proposed design, the calculated ECC value is 0.085 significantly below the threshold of 0.5, by the excitation of port 1 ensuring excellent diversity performance and minimizing signal correlation. DG quantifies the reduction in fading margin achieved by the antenna in a multiplexing system. The ideal value for DG is approximately 10 dB. The proposed antenna achieves DG values close to this ideal benchmark 9.19 dB by the excitation of port 1, validating its suitability for robust communication in multi-path environments. The DG is calculated by using Eq. (5).

$$DG = 10\sqrt{1 - |0.99\rho_{ij}|^2} \tag{5}$$

MEG is defined as the ratio of the average received power to the average incident power. Ideally, the MEG for a multiplexing antenna should be close to 0 dB to ensure balanced power distribution. The MEG of the proposed antenna aligns well with this ideal value -2.57 dB by the excitation of port 1, demonstrating balanced power reception among the antenna ports.

$$MEG_i = 0.5[1 - \sum_{j=1}^{N} |S_{ij}|^2] \tag{6}$$

TABLE 2. Performance comparison of SIW-based self-quadplexing antennas.

Ref	Type of Slot	Overall Size (λ_0^2)	Frequencies f_1, f_2, f_3, f_4 (GHz)	Minimum Isolation (dB)	Gain (dBi)	f_h/f_l (FR)	MES (λ_0)
[23]	Rectangular-slots	0.14	4.8, 5.4, 28, 30	20	5.4, 5.2, 8, 8.7	6.25	0.192
[27]	V-shaped slots	0.81	8.19, 8.8, 9.71, 11	22	5.5, 6.9, 7.47, 7.45	1.34	0.038
[24]	Rectangular-slots	0.2	3.5, 5.2, 5.5, 5.8	23.6	5.43, 4.10, 3.56, 3.6	1.65	0.051
[30]	T-shaped slots	0.31	8.85, 10.4, 11.4, 12.23	26	>6	1.38	0.534
[29]	Rectangular-slots	0.14	5.14, 5.78, 6.74, 7.74	28	4.1, 4.96, 6.2, 6.1	1.5	0.085
[28]	U-shaped slots	0.11	3.2, 4.1, 5.8, 7.2	30.5	5.8, 5.3, 3.9, 3.4	2.25	0.021
[26]	V-shaped slots	0.42	6.54, 7.64, 8.3, 9.6	30.5	5.8, 5.3, 3.9, 3.4	1.46	0.087
[22]	U-shaped slots	0.12	2.33, 2.96, 5.43, 6.15	32.5	4.21, 3.39, 6.1, 4.34	2.63	0.058
PW	Modified CSRR-inspired slots	0.037	2.09, 2.18, 2.26, 2.36	32.6	5.32, 5.58, 5.41, 5.18	1.13	0.013

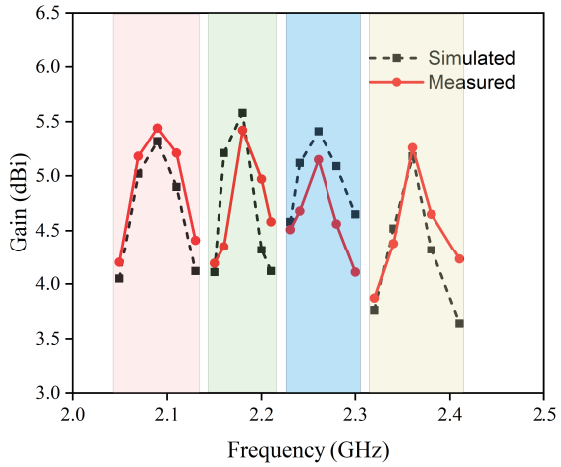

FIGURE 13. Simulated and measured gains of the self-quadplexing antenna.

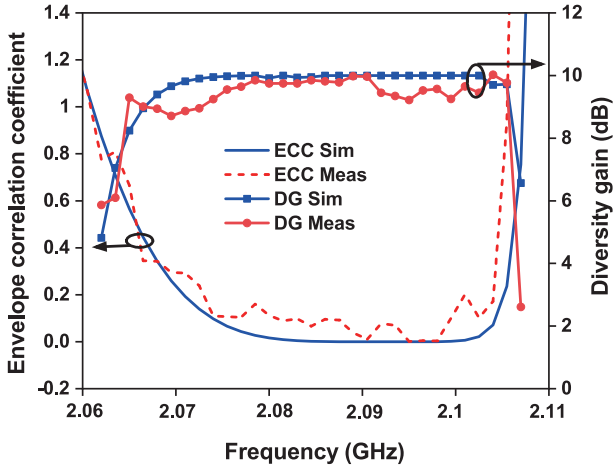

FIGURE 14. Simulated and measured ECC and DG of the self-quadplexing antenna.

A comparison of the performance of the proposed quadplexing antenna against other reported designs is provided in Table 2. In comparison, the antenna introduced in this work exceeds the performance metrics of other SIW-based quadplexing antennas.

5. CONCLUSION

This paper presents a self-quadplexing antenna that utilizes CSRR-inspired slots to facilitate quadplexing functionality. By varying the widths of these slots, the antenna resonates at four distinct frequencies: 2.09 GHz, 2.18 GHz, 2.26 GHz, and 2.36 GHz. The optimal position and configuration of the slots within the SIW structure provide minimal overlap, thereby reducing mutual coupling and enhancing port isolation. The antenna achieved a minimum port isolation of over 32.6 dB, with a compact footprint of $0.037\lambda_0^2$ and a frequency ratio of 1.13. Additionally, the antenna exhibits a gain greater than 5 dBi. The antenna's $|S|$-parameters and radiation patterns, derived from both simulations and measurements, demonstrate satisfactory performance. A notable advantage of the proposed quadplexing antenna is its capability for independent frequency tunability across the operational bands, positioning it as a suitable option for S-band applications.

REFERENCES

[1] Lokeshwar, B., D. Venkatasekhar, and A. Sudhakar, "Wideband low-profile SIW cavity-backed bilateral slots antenna for X-band application," *Progress In Electromagnetics Research M*, Vol. 97, 157–166, 2020.

[2] Chaturvedi, D. and S. Raghavan, "Compact QMSIW based antennas for WLAN/WBAN applications," *Progress In Electromagnetics Research C*, Vol. 82, 145–153, 2018.

[3] Chaturvedi, D. and A. Kumar, "A QMSIW cavity-backed self-diplexing antenna with tunable resonant frequency using CSRR slot," *IEEE Antennas and Wireless Propagation Letters*, Vol. 23, No. 1, 259–263, 2023.

[4] Gao, M., C. Liu, J. Nan, and H. Niu, "A broadband SIW cavity-backed circular arc-shaped slot antenna for millimeter-wave applications," *Progress In Electromagnetics Research Letters*, Vol. 117, 47–54, 2024.

[5] Lokeshwar, B., J. Ravindranadh, and D. Madhavi, "Design and analysis of a bandwidth enhanced low-profile SIW cavity-backed slot antenna using TE210 mode," *Progress In Electro-*

magnetics Research C., Vol. 125, 229–240, 2022.

[6] Kumar, A. and S. Raghavan, "Planar cavity-backed self-diplexing antenna using two-layered structure," *Progress In Electromagnetics Research Letters*, Vol. 76, 91–96, 2018.

[7] Bozzi, M., A. Georgiadis, and K. Wu, "Review of substrate-integrated waveguide circuits and antennas," *IET Microwaves, Antennas & Propagation*, Vol. 5, No. 8, 909–920, 2011.

[8] Deslandes, D. and K. Wu, "Single-substrate integration technique of planar circuits and waveguide filters," *IEEE Transactions on Microwave Theory and Techniques*, Vol. 51, No. 2, 593–596, 2003.

[9] Iqbal, A., I. B. Mabrouk, M. Al-Hasan, M. Nedil, and T. A. Denidni, "Wideband substrate integrated waveguide antenna for full-duplex systems," *IEEE Antennas and Wireless Propagation Letters*, Vol. 21, No. 1, 212–216, 2021.

[10] Deslandes, D. and K. Wu, "Accurate modeling, wave mechanisms, and design considerations of a substrate integrated waveguide," *IEEE Transactions on Microwave Theory and Techniques*, Vol. 54, No. 6, 2516–2526, 2006.

[11] Althuwayb, A. A., "Design of highly compact self-diplexing Y-shaped slot antenna employing quarter-mode substrate integrated waveguide," *International Journal of RF and Microwave Computer-Aided Engineering*, Vol. 31, No. 10, e22827, 2021.

[12] Pradhan, N. C., K. S. Subramanian, R. K. Barik, and Q. S. Cheng, "A shielded-QMSIW-based self-diplexing antenna for closely spaced bands and high isolation," *IEEE Antennas and Wireless Propagation Letters*, Vol. 20, No. 12, 2382–2386, 2021.

[13] Iqbal, A., M. Al-Hasan, I. B. Mabrouk, and M. Nedil, "Ultracompact quarter-mode substrate integrated waveguide self-diplexing antenna," *IEEE Antennas and Wireless Propagation Letters*, Vol. 20, No. 7, 1269–1273, 2021.

[14] Dash, S. K. K., Q. S. Cheng, R. K. Barik, N. C. Pradhan, and K. S. Subramanian, "A compact substrate integrated self-diplexing antenna for WiFi and ISM band applications," in *2020 50th European Microwave Conference (EuMC)*, 232–235, Utrecht, Netherlands, Jan. 2021.

[15] Barik, R. K., Q. S. Cheng, S. K. K. Dash, N. C. Pradhan, and S. S. Karthikeyan, "Compact high-isolation self-diplexing antenna based on SIW for C-band applications," *Journal of Electromagnetic Waves and Applications*, Vol. 34, No. 7, 960–974, 2020.

[16] Iqbal, A., J. J. Tiang, C. K. Lee, and N. K. Mallat, "SIW cavity backed self-diplexing tunable antenna," *IEEE Transactions on Antennas and Propagation*, Vol. 69, No. 8, 5021–5025, 2021.

[17] Iqbal, A., M. A. Selmi, L. F. Abdulrazak, O. A. Saraereh, N. K. Mallat, and A. Smida, "A compact substrate integrated waveguide cavity-backed self-triplexing antenna," *IEEE Transactions on Circuits and Systems II: Express Briefs*, Vol. 67, No. 11, 2362–2366, 2020.

[18] Priya, S. and S. Dwari, "A compact self-triplexing antenna using HMSIW cavity," *IEEE Antennas and Wireless Propagation Letters*, Vol. 19, No. 5, 861–865, 2020.

[19] Nigam, P., R. Agarwal, A. Muduli, S. Sharma, and A. Pal, "Substrate integrated waveguide based cavity-backed self-triplexing slot antenna for X-Ku band applications," *International Journal of RF and Microwave Computer-Aided Engineering*, Vol. 30, No. 4, e22172, 2020.

[20] Kumar, A., D. Chaturvedi, and S. Raghavan, "Low-profile substrate integrated waveguide (SIW) cavity-backed self-triplexed slot antenna," *International Journal of RF and Microwave Computer-Aided Engineering*, Vol. 29, No. 3, e21606, 2019.

[21] JayaPrakash, V. and D. S. Chandu, "Self-triplexing HMSIW antenna with enhanced isolation and extremely low frequency ratio," *AEU — International Journal of Electronics and Communications*, Vol. 170, 154829, 2023.

[22] Barik, R. K. and S. Koziel, "Highly miniaturized self-quadruplexing antenna based on substrate-integrated rectangular cavity," *IEEE Antennas and Wireless Propagation Letters*, Vol. 22, No. 3, 482–486, 2022.

[23] Naseri, H., P. PourMohammadi, A. Iqbal, A. A. Kishk, and T. A. Denidni, "SIW-based self-quadruplexing antenna for microwave and mm-wave frequencies," *IEEE Antennas and Wireless Propagation Letters*, Vol. 21, No. 7, 1482–1486, 2022.

[24] Kumar, A., "Design of self-quadruplexing antenna using substrate-integrated waveguide technique," *Microwave and Optical Technology Letters*, Vol. 61, No. 12, 2687–2689, 2019.

[25] JayaPrakash, V. and D. S. Chandu, "Self-isolated quadruplexing SIW antenna with extremely low frequency ratio for C-band applications," *Microwave and Optical Technology Letters*, Vol. 66, No. 2, 2024.

[26] Singh, A. K. and e. al., "Compact self-quadruplexing antenna based on SIW cavity-backed with enhanced isolation," *Progress In Electromagnetics Research C*, Vol. 110, 243–252, 2021.

[27] Priya, S., S. Dwari, K. Kumar, and M. K. Mandal, "Compact self-quadruplexing SIW cavity-backed slot antenna," *IEEE Transactions on Antennas and Propagation*, Vol. 67, No. 10, 6656–6660, 2019.

[28] Nigam, P. and V. Shenoy, "Self-quadplexing slot antenna for S- and C-band applications," *Telecommunications and Radio Engineering*, Vol. 82, No. 2, 17–30, 2023.

[29] Dash, S. K. K., Q. S. Cheng, and R. K. Barik, "A compact substrate integrated waveguide backed self-quadruplexing antenna for C-band communication," *International Journal of RF and Microwave Computer-Aided Engineering*, Vol. 30, No. 10, e22366, 2020.

[30] Kumar, K., S. Priya, S. Dwari, and M. K. Mandal, "Self-quadruplexing circularly polarized SIW cavity-backed slot antennas," *IEEE Transactions on Antennas and Propagation*, Vol. 68, No. 8, 6419–6423, 2020.

[31] Katta, A. K. and P. B. Choppala, "A compact four port high-isolation SIW-backed self-quadruplexing antenna with a swastik shaped slot for C band applications," *Progress In Electromagnetics Research C*, Vol. 143, 57–66, 2024.

[32] Chaturvedi, D., A. Kumar, A. A. Althuwayb, and F. Ahmadfard, "SIW-backed multiplexing slot antenna for multiple wireless system integration," *Electronics Letters*, Vol. 59, No. 11, e12826, 2023.

[33] Sharawi, M. S., A. T. Hassan, and M. U. Khan, "Correlation coefficient calculations for MIMO antenna systems: A comparative study," *International Journal of Microwave and Wireless Technologies*, Vol. 9, No. 10, 1991–2004, 2017.